ACS APPLIED MATERIALS & INTERFACES

Research Article

www.acsami.org

Poly(Lactic Acid) Hemodialysis Membranes with Poly(Lactic Acid)-*block*-Poly(2-Hydroxyethyl Methacrylate) Copolymer As Additive: Preparation, Characterization, and Performance

Lijing Zhu, Fu Liu, Xuemin Yu, and Lixin Xue*

Polymer and Composite Division, Key Laboratory of Marine Materials and Related Technologies, Zhejiang Key Laboratory of Marine Materials and Protective Technologies, Ningbo Institute of Materials Technology and Engineering, Chinese Academy of Sciences, Ningbo 315201, P.R. China

ABSTRACT: Poly(lactic acid) (PLA) hemodialysis membranes with enhanced antifouling capability and hemocompatibility were developed using poly(lactic acid)-*block*-poly(2-hydroxyethyl methacrylate) (PLA–PHEMA) copolymers as the blending additive. PLA–PHEMA block copolymers were synthesized via reversible addition–fragmentation (RAFT) polymerization from aminolyzed PLA. Gel permeation chromatography (GPC) and ^{1}H-nuclear magnetic resonance (^{1}H NMR) were applied to characterize the synthesized products. By blending PLA with the amphiphilic block copolymer, PLA/PLA–PHEMA membranes were prepared by nonsolvent induced phase separation (NIPS) method. Their chemistry and structure were characterized with X-ray photoelectron spectroscopy (XPS), scanning electron microscope (SEM) and atomic force microscopy (AFM). The results revealed that PLA/PLA–PHEMA membranes with high PLA–PHEMA contents exhibited enhanced hydrophilicity, water permeability, antifouling and hemocompatibility. Especially, when the PLA–PHEMA concentration was 15 wt %, the water flux of the modified membrane was about 236 L m^{-2} h^{-1}. Its urea and creatinine clearance was more than 0.70 mL/min, lysozyme clearance was about 0.50 mL/min, BSA clearance was as less as 0.31 mL/min. All the results suggest that PLA–PHEMA copolymers had served as effective agents for optimizing the property of PLA-based membrane for hemodialysis applications.

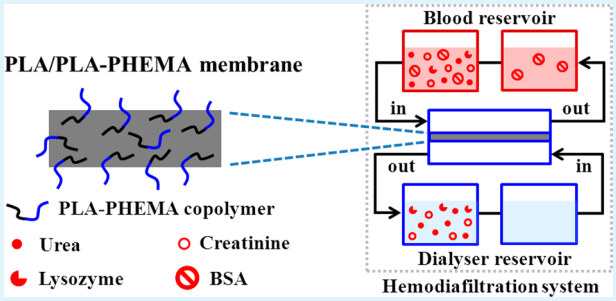

KEYWORDS: *poly(lactic acid), hemodialysis, hemocompatible, block copolymer, aminolysis*

INTRODUCTION

Worldwide, patients with chronic/acute kidney disease are increasing, for which hemodialysis is one of the most popular clinical therapies.[1−4] Conventional hemodialysis membranes are often prepared from petroleum-based nondegradable synthetic polymers such as poly(ether sulfone) (PES) and polysulfone (PSf) lacking biocompatibility and facing grave challenge in after-use waste disposal issues.[5,6] Recently, much attention has been paid to develop hemodialysis membranes made from biobased and biodegradable materials, such as poly(lactic acid) (PLA).[7]

Due to its biodegradability and biocompatibility, PLA is widely applied in food package, sutures, tissue engineering scaffolds and bone fixation.[8] However, in many applications, the serious challenge for PLA came from its hydrophobicity and biofouling.[9] Various techniques such as blending, self-assembly and surface grafting have been applied to introduce hydrophilicity to PLA matrix and surface.[10] Among the methods, blending modification is favored for its scalable capacity and higher efficiency. Polyethylene glycol (PEG), poly(ethylene oxide) (PEO), and poly(vinylpyrrolidone) (PVP) are the hydrophilic additives mostly used in the blending method. The hydrophilicity and antifouling of the PLA materials could be significantly improved initially by blending, but the blending hydrophilic additives may subject to loss during operation process because of their high water solubility.

In order to enhance the durability of the hydrophilicity and antifouling capacity of PLA materials, PEG-containing PLA amphiphilic block copolymers (PLA–PEG) have been synthesized and used as competitive additives.[11−15] Besides PLA–PEG, PLA amphiphilic block copolymers, such as PLA-*block*-poly(2-hydroxyethyl methacrylate) (PLA–PHEMA) and PLA-*block*-poly(N,N-dimethylaminoethyl methacrylate) (PLA–PDMAEMA), have been synthesized by ring opening polymerization (ROP) and controlled radical polymerization.[16−19] PHEMA is a favored hydrophilic polymer additive in biomedical field for its good biocompatibility.[20−22] However, PLA–PHEMA block copolymer has not been used as additive for PLA hemodialysis membranes modification yet.

In this Research Article, we attempted to enhance the hemocompatibility and antifouling performance of PLA hemodialysis membranes using PLA–PHEMA block copolymer as additive. PLA–PHEMA copolymer was synthesized from aminolyzed PLA chains via reversible addition–

Received: May 7, 2015
Accepted: July 29, 2015
Published: July 29, 2015

DOI: 10.1021/acsami.5b03951
ACS Appl. Mater. Interfaces 2015, 7, 17748−17755

fragmentation (RAFT) polymerization and incorporated into membrane-casting solution. Then PLA/PLA−PHEMA hemodialysis membranes were prepared via nonsolvent induced phase separation (NIPS) technology. The chemistry, morphology, hydrophilicity, permeability, antifouling, hemodialysis, and hemocompatibility of the prepared PLA membranes were researched in detail.

EXPERIMENTAL SECTION

Materials and Reagents. Poly(lactic acid) (PLA, 2002D) was bought from Natural Works. 2-Hydroxyethyl methacrylate (HEMA) was supplied by Aladdin and passed through a basic alumina column before use. Ethylenediamine (EDA), 4,6-dimethyl-2-pyridinamine (DMAP, 98%), *N*,*N*′-dicyclohexylcarbodiimide (DCC, 99%), poly(ethylene oxide) (PEO, M_v 100 000), bovine serum albumin (BSA, M_w = 67 000), creatinine, urea, and *p*-dimethylaminobenzaldehyde (PDAB) were purchased from Aladdin and used without further purification. Picric acid was bought from Sigma-Aldrich. RAFT agent of 4-cyano-4-(dodecylsulfanylthiocarbonyl)sulfanylpentanoic acid (CDP) was synthesized according to the previous literature.[23] Azobis(isobutyronitrile) (AIBN) was purchased from Shanghai Chemical Regent Company. Platelet-rich plasma (PRP) and platelet-poor plasma (PPP) were bought from Ningbo BioChance Co., Ltd., China. *N*,*N*′-dimethylformamide (DMF), tetrahydrofuran (THF), and ethanol were bought from Sinopharm Chemical Reagent Co., Ltd., China and used without other purification.

Synthesis of PLA−PHEMA Block Copolymer. In brief, the synthesis rout of PLA−PHEMA copolymers via RAFT polymerization included three steps: aminolysis reaction of PLA with EDA, synthesis of the macromolecular chain transfer agent and RAFT polymerization of HEMA.

In a typical aminolysis reaction, PLA (20 g) was dissolved in dioxane (180 mL). After the solution was stirred for 12 h at 30 °C, EDA (0.25 g) was added into the above PLA solution. After reaction for 5 min, the polymer solution was precipitated in water. The raw product was separated through filtration and thoroughly washed in water. The final product was obtained by freeze-drying for 24 h and named as PLA-EDA.

The macromolecular chain transfer agent (PLA-CDP) was synthesized via esterification/amination between the hydroxyl (−OH)/amino ($-NH_2$) groups of PLA-EDA and the carboxyl (−COOH) groups of CDP under the catalysis of DCC/DMAP. Briefly, PLA-EDA (15 g) was dissolved in THF (150 mL) under stirring. After 1 h, DCC (3.2 g, 15 mmol), DMAP (1.8 g, 15 mmol) and CDP (3.0 g, 10 mmol) were serially added into the mixture, and the amide reaction and esterification occurred at 20 °C. After it reacted for 24 h, the solution was precipitated and thoroughly washed in excessive ethanol. Then the solid product was collected through filtration and dried under vacuum at 40 °C.

The PLA−PHEMA block copolymer was synthesized by RAFT polymerization of HEMA. Briefly, PLA-CDP (2 g) was added into DMF (20 mL) under stirring in a three-neck flask. After 1 h, HEMA (3 g, 33.5 mmol) and AIBN (5 mg, 0.03 mmol) were added into the container and degassed with N_2 for additional 1.5 h at 20 °C. Then the flask was transferred to an oil bath at 70 °C, the RAFT polymerization of HEMA was carried out under N_2 protection and stirring. In 7 h, the reaction was ended by quenching with ice water. The solution was precipitated and washed in water. The solid PLA−PHEMA was obtained through filtration and dried via freeze-drying.

Preparation of the PLA/PLA−PHEMA Blend Membranes. PLA/PLA−PHEMA membranes were prepared via NIPS method as shown in previous report.[24] In a typical procedure, PLA, PLA−PHEMA, and PEO (7 g) were added into DMAc (73 g) under mechanical stirring at 80 °C for 12 h. After releasing bubbles under reduced pressure, the obtained casting solution was spread onto a polyester nonwoven fabric. They were immersed into a water bath at 30 °C for phase separation. After it was peeled from the substrate, it was removed and fully rinsed in distilled water. To avoid the shrinkage of membrane pores, the membrane was dried via freeze-drying. On the basis of the additive content, the fabricated PLA/PLA−PHEMA membranes were designated as M0, M5, M10, M15, and M20, respectively. The numbers in membrane ID denoted the corresponding weight percentages of PLA−PHEMA relative to the weight of PLA.

Characterization. ^{1}H NMR spectra was recorded on a Bruker Advance III spectrometer using DMSO-d_6 or $CDCl_3$ as the solvent and $Si(CH_3)_4$ as an internal standard at room temperature. Gel permeation chromatography (GPC) was conducted using the modular instrument as shown in the previous work.[25] Membrane morphologies were characterized by field emitting scanning electronic microscopy (SEM, Hitachi S-4800, Japan). Cross-sectional samples of the membranes were made by snapping them in liquid nitrogen. Prior to experiments, the membrane samples were sputtered (Hitachi E-1045 Ion Sputter, Japan) with platinum at an argon pressure of 0.1 Torr for 120 s at a current of 10 mA. Atomic force microscopy (AFM, Dimension3100 V, Veeco, US) images were collected under the tapping mode with silicon tip cantilevers. The root-mean-square (RMS) was calculated. The given data were averaged from three measurements. Membrane surface chemistry was detected by X-ray photoelectron spectroscopy (XPS, PHI-5000C ESCA System, US) with Mg Kα excitation radiation ($h\nu$ = 1253.6 eV). The takeoff angle of the photoelectron was set to 30°, 60°, and 90°, respectively. More details of XPS experiment has been described in the reference.[26] The given elemental atomic percentages were averaged from three different samples.

Hydrophilicity. Water contact angle (WCA) was used to characterize the hydrophilicity of the prepared membranes. It carried out on a contact angle measurement (OCA20, Data physics, Germany) under the sessile mode. A piece of membrane (1.5 × 5.0 cm) was mounted on the sample holder. A double distilled water droplet (volume = 1.0 μL) was suspended from the tip of a microsyringe and then moved downward to touch the membrane surface. The sessile water droplet attached on the surfaces, the water contact angle varying with time was recorded by video. The given data were averaged from three different samples, with at least three locations on a single sample measured. During experiment, the temperature and relative humidity was maintained at 20 °C and 70%, respectively.

Filtration and Antifouling Properties. The filtration and antifouling ability of the membranes was assessed using a stirred filtration cell (Millipore Corporation, XFUF04701, US) according to the previous reports.[25,27] Typically, a circular membrane sample was fixed on the sample holder in the cell. Then pure water was pressed through the membrane under 0.1 MPa. The permeate liquid was consecutively collected and weighted. The flux (J) can be calculated according to eq 1 until the value was stable, and the stable water flux was denoted as J_1. Subsequently, 1.0 g/L BSA solution was pressed through the same membrane. The BSA flux was consecutively calculated and the stable value was named as J_2. After BSA solution filtration, the membrane was taken out and shaken in PBS buffer solution (pH 7.4) for 24 h. Finally, water was again pushed through the cleaned membrane, and the obtained stable water flux was named as J_3. During the experiment, the temperature of the liquid was kept at 37 °C. All given data were averaged from three different measurements.

$$J = \frac{V}{S \times t} \tag{1}$$

where J (L/m^2 h) is the flux, V (L) is the volume of the collected liquid, S (1.77×10^{-3} m^2) is the sample area, and t (h) is the filtration time, respectively.

The flux recovery ratio (FRR) and total fouling (F_t) parameters were calculated by the following eqs 2 and 3, respectively. Specifically, F_t is divided into reversible fouling ($F_r = (J_3 - J_2)/J_1$) and irreversible fouling ($F_{ir} = (J_1 - J_3)/J_1$). The percentages of F_r and F_{ir} in F_t (F_r/F_t and F_{ir}/F_t) have been calculated. All given values were averaged from three different measurements.

$$\mathrm{FRR} = \frac{J_3}{J_1} \times 100\% \tag{2}$$

DOI: 10.1021/acsami.5b03951
ACS Appl. Mater. Interfaces 2015, 7, 17748−17755

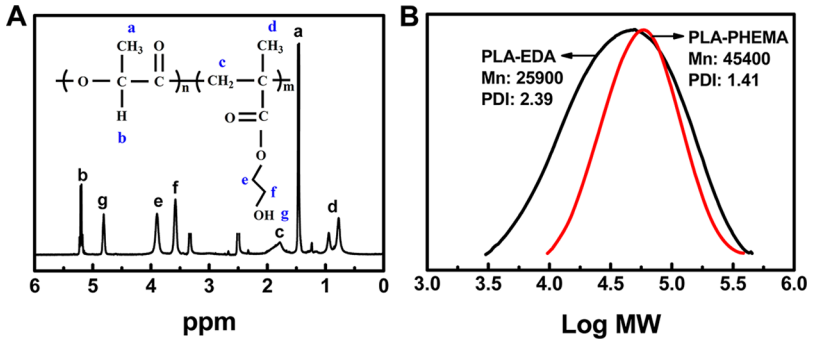

Figure 1. (A) ^{1}H NMR spectrum of PLA−PHEMA in DMSO-d_6. (B) GPC traces of PLA−EDA and PLA−PHEMA.

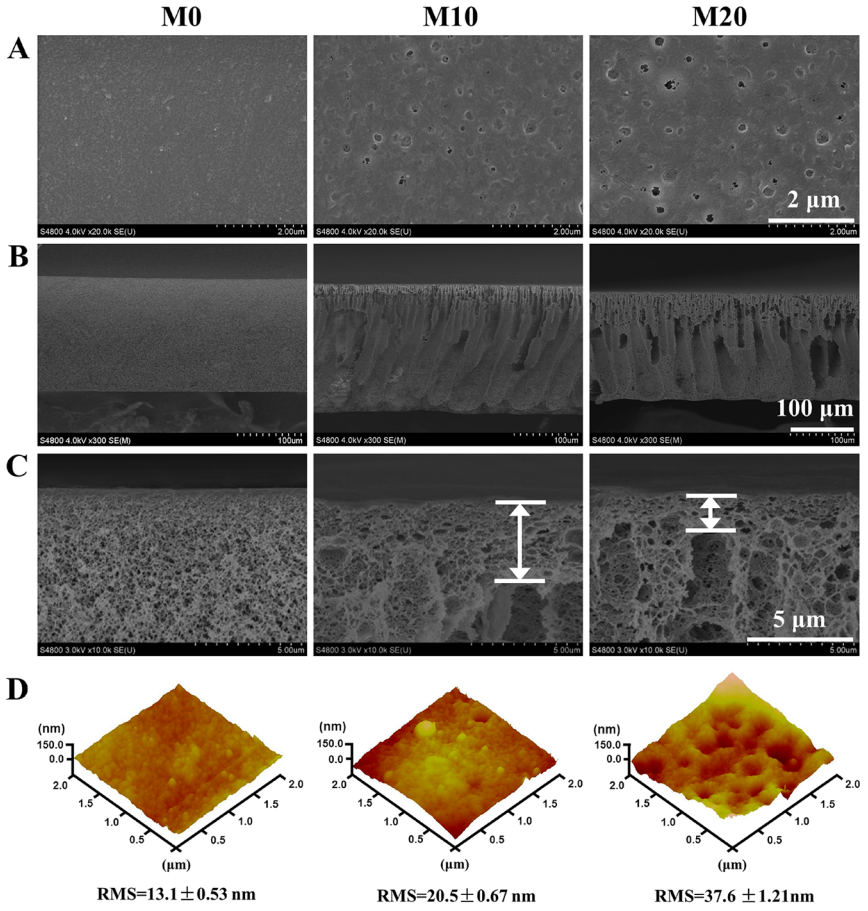

Figure 2. (A) Open side surface SEM images of the membranes. (B) The cross-section SEM images of the membranes. (C) The enlarged cross-section SEM images of the membranes. (D) AFM topographies of the pure PLA (M0) and PLA/PLA−PHEMA blend membranes (M10 and M20). Data were means ± SD (n = 3).

$$F_t = \frac{J_1 - J_2}{J_1} \quad (3)$$

Hemodialysis Simulation Experiment. Hemodialysis ability of the membranes was characterized with clearance of urea (Clearance$_{Urea}$), creatinine (Clearance$_{Creatinine}$), and lysozyme (Clearance$_{Lysozyme}$) at 37 °C. The solution of urea (1.5 g/L), creatinine (0.1 g/L), and lysozyme (0.2 g/L) in physiological saline (0.9 wt %) was used as mimic blood, and distilled water was used as dialysate. They traversed through the dialysis mode in the opposite direction at a speed of 100 and 300 mL/min, respectively. The effective membrane area was 29.2 cm^2. In 6 h, the solution was taken out from the outlet of the mimic blood solution. The clearance of urea, creatinine, and lysozyme were calculated according to eq 4.[28] Similarly, BSA clearance (Clearance$_{BSA}$) was measured using BSA solution (1 g/L) as feed. Three samples of each membrane were investigated and each given value was an average of three measurements.

$$\text{Clearance (mL/min)} = Q_{Bi}\frac{C_{Bi} - C_{Bo}}{C_{Bi}} + Q_{UF}\frac{C_{Bo}}{C_{Bi}} \quad (4)$$

where Q_{Bi} and Q_{UF} (mL/min) are the blood inlet and ultrafiltration flow, respectively. C_{Bi} and C_{Bo} are the mimic blood inlet and outlet concentrations, respectively. The urea concentration was determined through the colorimetric assay of urea and PDAB at a wavelength of 440 nm. The creatinine concentration was determined through the colorimetric assay of creatinine and picric acid at a wavelength of 510 nm. The lysozyme and BSA concentration was determined with a UV−vis spectrophotometer at the wavelength of 280 nm, respectively.

DOI: 10.1021/acsami.5b03951
ACS Appl. Mater. Interfaces 2015, 7, 17748−17755

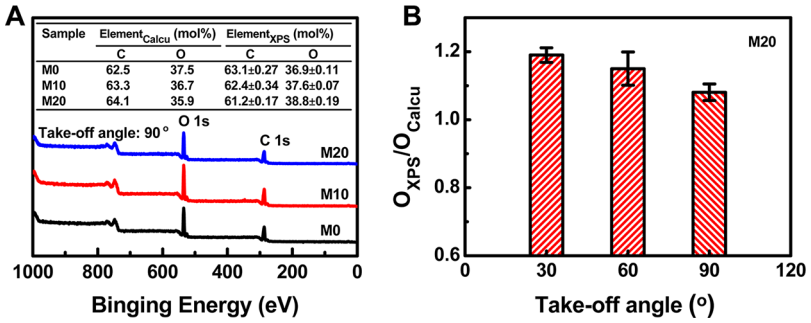

Figure 3. (A) XPS wide scans with a takeoff angle of 90° of the PLA membrane (M0) and typical PLA/PLA−PHEMA membranes (M10 and M20). (B) O_{XPS}/O_{Calcu} ratios of M20 with takeoff angles of 30°, 60°, and 90°, respectively. Data were means ± SD (n = 3).

Protein Adsorption. Each rinsed membrane sample with an area of 12.5 cm^2 was equilibrated at 37 °C for 1 h. It was then immersed into a vial filled with BSA solution (10 mL, 1 g/L). Subsequently, the vial was incubated at water bath at 37 °C for 8 h. Then the sample was carefully rinsed with PBS buffer solution (pH 7.4) to remove unstable BSA. The amount of adsorbed BSA (Adsorption$_{BSA}$) on membrane sample was calculated according to the eq 5

$$\text{Adsorption}_{BSA}\ (\mu g/cm^2) = \frac{C_{before} - C_{after}}{S} \quad (5)$$

where C_{before} and C_{after} represent the BSA concentration before and after treating with membrane sample. S (12.5 cm^2) is the membrane sample area. The given value was averaged from three different measurements.

Platelet Adhesion. In brief, round membrane samples (d = 1 cm) were put into 24-well plate. 100 μL platelet-rich plasma (PRP) was carefully added onto each membrane and kept at 37 °C for 1 h. Afterward, the membrane was washed with PBS buffer solution (pH 7.4) and immersed into 5 wt % glutaraldehyde solution for 2 h. Next the sample was washed with ultrapure water and dehydrated using ethanol/water solutions (10, 30, 50, 70, 90, 100 wt %). The dried membranes were observed with SEM (Hitachi S-4800, Japan) after sputtering a platinum layer. For a membrane, five samples were subjected to the experiment and detected by SEM. The number of the platelets absorbed on membrane surfaces ($N_{Platelet}$) was counted. The given value was averaged from five measurements.

Plasma Recalcification Time (PRT). Platelet-poor plasma (PPP, 100 μL, 37 °C) was dropped to membrane surface and incubated at 37 °C for 1 min. Then $CaCl_2$ aqueous solution (100 μL, 0.05 M) was dropped to the membrane sample. They were stirred gently. Plasma recalcification time (PRT) was the time once the first fibrin strand formed. Each PRT value was averaged from six measurements.

RESULTS AND DISCUSSION

Characterization of the Synthesized PLA−PHEMA Copolymer. During the aminolysis reaction of PLA with EDA, EDA acted as a nucleophile and attacked PLA at the electron deficient center —C═O, endowing the shorter PLA chains with −NH_2 and −OH groups. The reactive groups were used as sites to further immobilize RAFT agent CDP, which were employed as the macromolecular chain transfer agent to regulate RAFT polymerization of HEMA. PLA−PHEMA was characterized by ^{1}H NMR as shown in Figure 1A. Seen from Figure 1A, signals in the 5.19−5.14 (a) and 1.59−1.57 ppm range (b) belonged to −CH− and −CH_3 protons of the main chain PLA units. And the peaks in 1.8 (c) and 0.77−0.94 ppm range (d) were attributed to −CH_2− and −CH_3 protons of the main chain PHEMA units. The peaks in 3.6 (f) and 3.9 ppm (e) were the signals of −CH_2 protons connecting with −OH (4.88 ppm, g) and ester groups of PHEMA, respectively. The GPC diagrams of PLA−EDA and PLA−PHEMA (Figure 1B) exhibited a monomodal distribution. The number-average molecular weight (M_n) of the products elevated from 25900 (PLA−EDA) to 45400 g/mol (PLA−PHEMA). According to the ^{1}H NMR and GPC results, PLA−PHEMA block copolymer had been successful synthesized via RAFT polymerization. The PLA−PHEMA block copolymer was then used as additive to modify PLA hemodialysis membranes.

Membrane Morphologies. The effects of PLA−PHEMA addition on the morphologies of the PLA blend membranes (M10 and M20) were characterized with SEM and AFM. Their typical images are shown in Figure 2. From Figure 2A, the open side surface of the pure PLA membrane (M0) was quite dense and smooth. The pore size and porosity significantly increased upon addition of PLA−PHEMA. Larger pores had been observed for M10 and M20. From Figure 2B, the cross-session morphologies of the PLA/PLA−PHEMA membranes were quite different from pure PLA membrane. For the pure PLA membrane, spongy structure was observed throughout the cross-section image. But PLA/PLA−PHEMA membranes had dense skin layer and finger-like pores. From the enlarged cross-section images (Figure 2C), the skin layer thickness of the blend membranes was falled from 3.6 ± 0.17 (M10) to 1.7 ± 0.11 μm (M20). This result agreed with what had been reported that the amphiphilic additive enhanced phase separation and improved finger-like pores formation.[29,30] The surfaces of PLA/PLA−PHEMA membranes were also characterized by AFM. According to Figure 2D, the root-mean-square (RMS) values of the PLA/PLA−PHEMA membranes were higher than that of pure PLA membrane (13.1 ± 0.53 nm). As the PLA−PHEMA additive increased, the RMS value increased from 20.5 ± 0.67 (M10) to 37.6 ± 1.21 nm (M20). The evolution of the membrane pores and roughness was attributed to the pore-forming behavior of the hydrophilic PHEMA in the block copolymer additive.

Membrane Surface Composition. XPS spectra and elemental mole percentages of the membranes are shown in Figure 3. In Figure 3A, both the pure PLA membrane (M0) and PLA/PLA−PHEMA membranes (M10 and M20) had carbon (C) and oxygen (O) peaks. The elemental mole percentage detected by XPS was defined as Element$_{XPS}$. On the other hand, the elemental concentration calculated on the basis of the membrane composition and molecular structures of PLA and PLA−PHEMA was correspondingly named as Element$_{Calcu}$. The data were also shown in Figure 3A. With the increase of PLA−PHEMA concentration, the O elemental percentage detected by XPS (O_{XPS}) of the modified membranes increased from 37.6 ± 0.07 (M10) to 38.8 ± 0.19% (M20), while, the calculated O elemental percentage (O_{Calcu}) of the membranes

DOI: 10.1021/acsami.5b03951
ACS Appl. Mater. Interfaces 2015, 7, 17748−17755

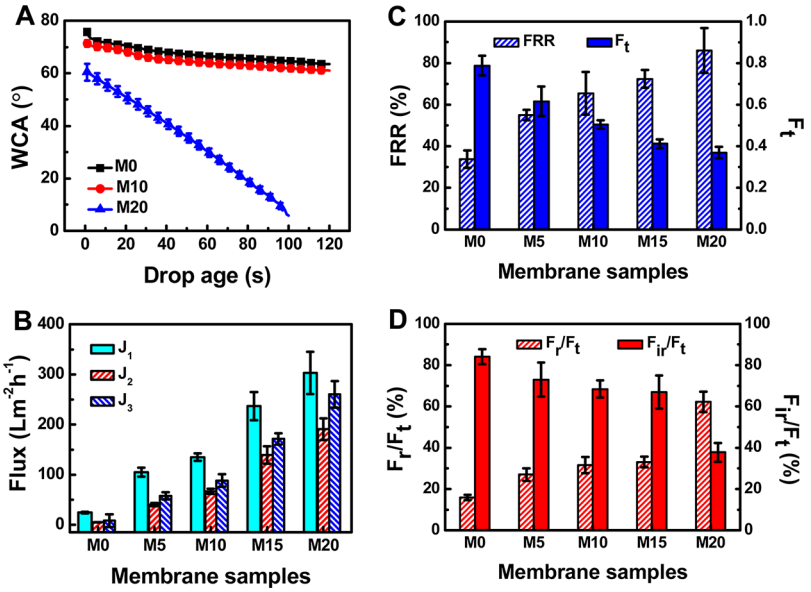

Figure 4. (A) The orbits of water contact angle (WCA) attenuating with the elongation of time for the pure PLA membrane (M0) and typical PLA/PLA−PHEMA membranes (M10 and M20). Data were means ± SD (n = 9). (B) Pure water flux (J_1), BSA solution flux (J_2), and recovery pure water flux (J_3) of the membranes. (C) Water flux recovery ratio (FRR) and total fouling (F_t) of the membranes. (D) The ratio of reversible fouling (F_r) and irreversible fouling (F_{ir}) to the total fouling (F_r/F_t and F_{ir}/F_t), respectively. Data were means ± SD (n = 3).

decreased from 36.7 (M10) to 35.9% (M20). This suggested that the more additive added, the more PHEMA chains enriched on the membrane surfaces. The enrichment of PHEMA chains on surface of M20 was also confirmed by the surface elemental percentages with different takeoff angle. As shown in Figure 3B, O_{XPS}/O_{Calcu} ratios decreased with the increasing takeoff angle. The larger the takeoff angle of XPS is given, the deeper the detecting depth becomes.[27] All the results indicated that PHEMA chains from the PLA−PHEMA copolymers migrated to the skin layer of the membrane. The behavior was known as surface segregation of amphiphilic block copolymers.[31,32]

Hydrophilicity and Antifouling. Water contact angle (WCA) for hydrophilic membranes often attenuates with the elongation of drop age because of the pores and chemical structures of the surfaces. The orbits of WCA for the membranes are shown in Figure 4A. The initial WCA of the pure PLA membrane (M0) was as high as 75.8°. PLA/PLA−PHEMA membranes exhibited reduced WCA from about 71.4° (M10) to 60.5° (M20). In addition, WCA of M20 rapidly attenuated to 10° within 100 s. The results suggested that PLA/PLA−PHEMA membranes exhibited improved hydrophilicity because of the hydroxyl groups of PHEMA on membrane surfaces and pore walls as mentioned in last section.

Nonspecific protein adsorption in dynamic permeation experiments with BSA is a conventional way to assess the antifouling properties of the membranes. Generally, in one cycle of dynamic filtration, pure water, BSA solution and pure water were pushed through the membrane samples, and the three fluxes (J_1, J_2, and J_3) were recorded successively. In this work, Figure 4B showed the three fluxes of the pure PLA membrane (M0) and PLA/PLA−PHEMA membranes (M5, M10, M15, and M20). It is clear that PLA/PLA−PHEMA membranes had a higher J_1 than that of the pure PLA membrane. Moreover, J_1 increased from 104.9 (M5) to 302.8 L m^{-2} h^{-1} (M20) with the increase of PLA−PHEMA concentrations in the membranes. The results were ascribed to the increase in pore size and hydrophilicity of the membranes by incorporating PLA−PHEMA block copolymer as additive. As seen from Figure 4B, J_2 of each membrane sample was significantly lower than its J_1. During the filtration process of BSA solution, BSA molecules aggregated and covered on membrane surfaces leading to membrane fouling and lower flux.[33] After washed for 12 h, J_3 of the cleaned membranes was larger than J_2 for the same membrane. The results suggested that membrane fouling could be eliminated in some degree by water cleaning. On the basis of the obtained fluxes, water flux recovery ratio (FRR) and total fouling (F_t) of the PLA membranes were calculated and given in Figure 4C. Compared with M0 (33.8%), FRR for the PLA/PLA−PHEMA membranes was improved from 54.9 (M5) to 86.0% (M20). Moreover, the PLA/PLA−PHEMA membranes exhibited decreased F_t and increased F_r/F_t indicating enhanced antifouling property upon modification with more PLA−PHEMA additive. It is mainly attributed to the hydrophilicity of PHEMA chains. Usually, it is more difficult to form BSA cake on hydrophilic membrane surfaces than hydrophobic ones.[24] As a result, hydrophilic membranes often show better antifouling capability.

Hemodialysis. The pure PLA membrane (M0) and PLA/PLA−PHEMA membranes (M5, M10, M15, and M20) were subjected to hemodialysis tests. In this work, a solution of urea, creatinine, lysozyme, and BSA was used as mimic blood. The clearance of urea ($Clearance_{Urea}$), creatinine ($Clearance_{Creatinine}$), lysozyme ($Clearance_{Lysozyme}$), and BSA ($Clearance_{BSA}$) are summerized in Figure 5. For the small molecules of urea and creatinine, all PLA membranes exhibited similar $Clearance_{Urea}$ (0.78 mL/min) and $Clearance_{Creatinine}$ (0.74 mL/min). For the middle molecule of lysozyme and large molecule of BSA, $Clearance_{Lysozyme}$ and $Clearance_{BSA}$ of the PLA/PLA−PHEMA membranes was increased with the increase of PLA−PHEMA concentration in the membranes with increased pore size (see Figure 2A). In fact, during hemodialysis, it is necessary to thoroughly eliminate small and middle molecules such as

DOI: 10.1021/acsami.5b03951
ACS Appl. Mater. Interfaces 2015, 7, 17748−17755

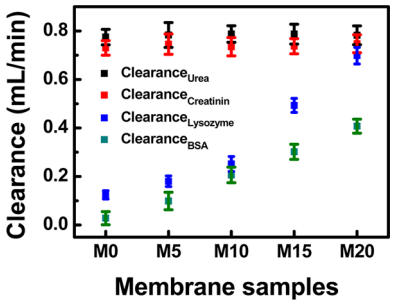

Figure 5. Urea clearance ($Clearance_{Urea}$), creatinine clearance ($Clearance_{Creatinine}$), lysozyme clearance ($Clearance_{Lysozyme}$), and BSA clearance ($Clearance_{BSA}$) of the pure PLA membrane (M0) and PLA/PLA−PHEMA blend membranes (M5, M10, M15, and M20). Data were means ± SD (n = 3).

urea, creatinine and lysozyme, but, it has to prevent the loss of beneficial plasma proteins.[34] Therefore, in consideration of the flux and solute clearance, M15 was preferred, in which the water flux was 236.7 L m^{-2} h^{-1}, both $Clearance_{Urea}$ and $Clearance_{Creatinine}$ were more than 0.70 mL/min, $Clearance_{Lysozyme}$ was about 0.50 mL/min, and $Clearance_{BSA}$ was about 0.31 mL/min.

Hemocompatibility. During hemodialysis process, proteins and platelets are able to absorb and deposit onto membrane surfaces leading to seriously complications. Therefore, the hemocompatibility of the hemodialysis membrane is one of the vital factors. In this work, BSA adsorption, platelet adhesion, and plasma recalcification time (PRT) of the membranes were characterized and the results are shown in Figure 6. It is clear that $Adsorption_{BSA}$ of the membranes decreased and PRT of them increased from M0 to M20, indicating reduced BSA adsorption and prolonged plasma recalcification time. In addition, the pseudopodia of the adhered platelets on PLA/PLA−PHEMA membrane surfaces gradually disappeared. Meanwhile, $N_{Platelet}$ on membrane surfaces decreased from M0 to M20, suggesting suppressed platelet adhesion and activation. All the results indicated the hemocompatibility of the PLA membrane was significantly improved by introducing PLA−PHEMA block copolymers as additive, which was mainly attributed to the improved hydrophilicity of the PLA/PLA−PHEMA membranes. The hydroxyl-rich PLA/PLA−PHEMA membranes can suppress the formation of thrombus.[35]

CONCLUSIONS

PLA−PHEMA block copolymer was synthesized via RAFT polymerization and used as the hydrophilic additive to modify PLA membranes via NIPS method. The PLA/PLA−PHEMA membranes exhibited improved hydrophilicity, leading to better hemocompatibility (low BSA adsorption, prolonged plasma recalcification times and suppressed platelet adhesion) and antifouling properties (higher water flux recovery ratio and lower total fouling). Maintaining excellent urea and creatinine clearance, the increase of PLA−PHEMA in the membranes also increased lysozyme and BSA clearance. Balancing the need to eliminate small/middle molecules and retain big proteins, M15 with 15 wt % of PLA−PHEMA additive seems to be preferred for practical application. This research offers an effective way to enhance the antifouling, hemocompatibility, permeation, and selectivity of the PLA hemodialysis membranes.

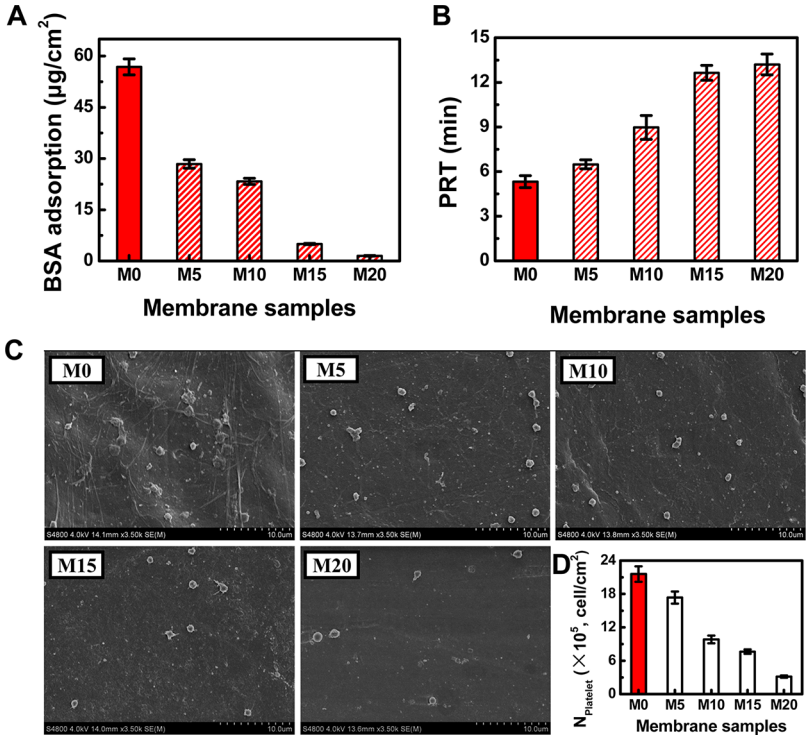

Figure 6. Hemocompatibility of the pure PLA membrane (M0) and PLA/PLA−PHEMA blend membranes (M5, M10, M15, and M20). (A) The amount of adsorbed BSA ($Adsorption_{BSA}$) on the membranes. Data were means ± SD (n = 3). (B) The plasma recalcification time (PRT) for the pure PLA and PLA/PLA−PHEMA blend membranes. Data were means ± SD (n = 6). (C) The typical SEM images of the adherent platelets on the membrane surfaces. (D) The number of the adherent platelets ($N_{Platelet}$) on the surfaces of membrane. Data were means ± SD (n = 5).

DOI: 10.1021/acsami.5b03951
ACS Appl. Mater. Interfaces 2015, 7, 17748−17755

AUTHOR INFORMATION

Corresponding Author

*E-mail: xuelx@nimte.ac.cn.

Notes

The authors declare no competing financial interest.

ACKNOWLEDGMENTS

This work is financed by the National Natural Science Foundation of China (No. 51473177), Ningbo Science and Technology Bureau (No. 2014B81004), the National Natural Science Foundation of Ningbo (No. 2014A610141), and the Zhejiang Province Preferential Postdoctoral Funded Project (No. BSH1402075).

REFERENCES

(1) Ariyaratne, T. V.; Ademi, Z.; Duffy, S. J.; Andrianopoulos, N.; Billah, B.; Brennan, A. L.; New, G.; Black, A.; Ajani, A. E.; Clark, D. J.; Yan, B. P.; Yap, C.-H.; Reid, C. M. Cardiovascular Readmissions and Excess Costs Following Percutaneous Coronary Intervention in Patients with Chronic Kidney Disease: Data from a Large Multi-Centre Australian Registry. *Int. J. Cardiol.* **2013**, *168*, 2783−2790.

(2) Xiong, G.; Chen, X.; Li, X.; Fang, D.; Zhang, L.; Yang, L.; Zhang, L.; Yao, L.; He, Z.; Zhou, L. Prevalence and Factors Associated with Baseline Chronic Kidney Disease in China: A 10-Year Study of 785 Upper Urinary Tract Urothelial Carcinoma Patients. *J. Formosan Med. Assoc.* **2014**, *113*, 521−526.

(3) Sugiyama, H.; Yokoyama, H.; Sato, H.; Saito, T.; Kohda, Y.; Nishi, S.; Tsuruya, K.; Kiyomoto, H.; Iida, H.; Sasaki, T.; Higuchi, M.; Hattori, M.; Oka, K.; Kagami, S.; Kawamura, T.; Takeda, T.; Hataya, H.; Fukasawa, Y.; Fukatsu, A.; Morozumi, K.; Yoshikawa, N.; Shimizu, A.; Kitamura, H.; Yuzawa, Y.; Matsuo, S.; Kiyohara, Y.; Joh, K.; Nagata, M.; Taguchi, T.; Makino, H. Japan Renal Biopsy Registry and Japan Kidney Disease Registry: Committee Report for 2009 and 2010. *Clin. Exp. Nephrol.* **2013**, *17*, 155−173.

(4) Ahn, C.; Koo, T. Y.; Jeong, J. C.; Kim, M.; Yang, J.; Lee, J.; Min, S. I.; Lee, J. E.; Kim, M. S.; Kwon, O. J.; Kim, S. J.; Kim, Y. H.; Kim, Y. H.; Choi, B. S.; Choi, S. J. N.; Lee, D. H.; Chung, S. Y.; Cho, W. H.; Kim, Y. S. Initial Report of the Korean Organ Transplant Registry: The First Report of National Kidney Transplantation Data. *Transplant. Proc.* **2014**, *46*, 425−430.

(5) Xiang, T.; Luo, C. D.; Wang, R.; Han, Z. Y.; Sun, S. D.; Zhao, C. S. Ionic-Strength-Sensitive Polyethersulfone Membrane with Improved Anti-Fouling Property Modified by Zwitterionic Polymer Via in Situ Cross-Linked Polymerization. *J. Membr. Sci.* **2015**, *476*, 234−242.

(6) Wang, L.; Wang, J.; Gao, X.; Liang, Z.; Zhu, B.; Zhu, L.; Xu, Y. A Facile Transetherification Route to Polysulfone-Poly(Ethylene Glycol) Amphiphilic Block Copolymers with Improved Protein Resistance. *Polym. Chem.* **2014**, *5*, 2836−2842.

(7) Madhavan Nampoothiri, K.; Nair, N. R.; John, R. P. An Overview of the Recent Developments in Polylactide (Pla) Research. *Bioresour. Technol.* **2010**, *101*, 8493−8501.

(8) Lasprilla, A. J.; Martinez, G. A.; Lunelli, B. H.; Jardini, A. L.; Filho, R. M. Poly-Lactic Acid Synthesis for Application in Biomedical Devices - a Review. *Biotechnol. Adv.* **2012**, *30*, 321−328.

(9) Oh, J. K. Polylactide (Pla)-Based Amphiphilic Block Copolymers: Synthesis, Self-Assembly, and Biomedical Applications. *Soft Matter* **2011**, *7*, 5096−5108.

(10) Rasal, R. M.; Janorkar, A. V.; Hirt, D. E. Poly(Lactic Acid) Modifications. *Prog. Polym. Sci.* **2010**, *35*, 338−356.

(11) Zhang, X.; Chen, D.; Ba, S.; Zhu, J.; Zhang, J.; Hong, W.; Zhao, X.; Hu, H.; Qiao, M. Poly(L-Histidine) Based Triblock Copolymers: Ph Induced Reassembly of Copolymer Micelles and Mechanism Underlying Endolysosomal Escape for Intracellular Delivery. *Biomacromolecules* **2014**, *15*, 4032−4045.

(12) Ma, C.; Pan, P.; Shan, G.; Bao, Y.; Fujita, M.; Maeda, M. Core-Shell Structure, Biodegradation, and Drug Release Behavior of Poly(Lactic Acid)/Poly(Ethylene Glycol) Block Copolymer Micelles Tuned by Macromolecular Stereostructure. *Langmuir* **2015**, *31*, 1527−1536.

(13) Stover, R. J.; Murthy, A. K.; Nie, G. D.; Gourisankar, S.; Dear, B. J.; Truskett, T. M.; Sokolov, K. V.; Johnston, K. P. Quenched Assembly of Nir-Active Gold Nanoclusters Capped with Strongly Bound Ligands by Tuning Particle Charge Via Ph and Salinity. *J. Phys. Chem. C* **2014**, *118*, 14291−14298.

(14) Moriya, A.; Shen, P.; Ohmukai, Y.; Maruyama, T.; Matsuyama, H. Reduction of Fouling on Poly(Lactic Acid) Hollow Fiber Membranes by Blending with Poly(Lactic Acid)−Polyethylene Glycol−Poly(Lactic Acid) Triblock Copolymers. *J. Membr. Sci.* **2012**, *415−416*, 712−717.

(15) Shen, P.; Moriya, A.; Rajabzadeh, S.; Maruyama, T.; Matsuyama, H. Improvement of the Antifouling Properties of Poly (Lactic Acid) Hollow Fiber Membranes with Poly (Lactic Acid)−Polyethylene Glycol−Poly (Lactic Acid) Copolymers. *Desalination* **2013**, *325*, 37−39.

(16) Bolton, J.; Rzayev, J. Synthesis and Melt Self-Assembly of Ps−Pmma−Pla Triblock Bottlebrush Copolymers. *Macromolecules* **2014**, *47*, 2864−2874.

(17) Viswanathan, P.; Themistou, E.; Ngamkham, K.; Reilly, G. C.; Armes, S. P.; Battaglia, G. Controlling Surface Topology and Functionality of Electrospun Fibers on the Nanoscale Using Amphiphilic Block Copolymers to Direct Mesenchymal Progenitor Cell Adhesion. *Biomacromolecules* **2015**, *16*, 66−75.

(18) Akimoto, J.; Nakayama, M.; Sakai, K.; Okano, T. Temperature-Induced Intracellular Uptake of Thermoresponsive Polymeric Micelles. *Biomacromolecules* **2009**, *10*, 1331−1336.

(19) Wolf, F. F.; Friedemann, N.; Frey, H. Poly(Lactide)-Block-Poly(Hema) Block Copolymers: An Orthogonal One-Pot Combination of Rop and Atrp, Using a Bifunctional Initiator. *Macromolecules* **2009**, *42*, 5622−5628.

(20) Tanaka, M.; Mochizuki, A. Clarification of the Blood Compatibility Mechanism by Controlling the Water Structure at the Blood-Poly(Meth)Acrylate Interface. *J. Biomater. Sci., Polym. Ed.* **2010**, *21*, 1849−1863.

(21) Jaiswal, M.; Koul, V. Assessment of Multicomponent Hydrogel Scaffolds of Poly(Acrylic Acid-2-Hydroxy Ethyl Methacrylate)/Gelatin for Tissue Engineering Applications. *J. Biomater. Appl.* **2013**, *27*, 848−861.

(22) Bayramoglu, G.; Can Akcalı, K.; Gultekin, S.; Bengu, E.; Arica, M. Y. Preparation and Characterization of Poly(Hydroxyethyl Methacrylate-Co -Poly(Ethyleneglycol-Methacrylate)/Hydroxypropyl-Chitosan) Hydrogel Films: Adhesion of Rat Mesenchymal Stem Cells. *Macromol. Res.* **2011**, *19*, 385−395.

(23) Moad, G.; Chong, Y. K.; Postma, A.; Rizzardo, E.; Thang, S. H. Advances in Raft Polymerization: The Synthesis of Polymers with Defined End-Groups. *Polymer* **2005**, *46*, 8458−8468.

(24) Zhu, L. J.; Liu, F.; Yu, X. M.; Gao, A. L.; Xue, L. X. Surface Zwitterionization of Hemocompatible Poly(Lactic Acid) Membranes for Hemodiafiltration. *J. Membr. Sci.* **2015**, *475*, 469−479.

(25) Zhu, L. J.; Zhu, L. P.; Zhao, Y. F.; Zhu, B. K.; Xu, Y. Y. Anti-Fouling and Anti-Bacterial Polyethersulfone Membranes Quaternized from the Additive of Poly(2-Dimethylamino Ethyl Methacrylate) Grafted Sio2nanoparticles. *J. Mater. Chem. A* **2014**, *2*, 15566−15574.

(26) Tian, Y.; Ye, S.; Ran, Q.; Xian, Y.; Xu, J.; Peng, R.; Jin, L. Generation of Surface-Confined Catechol Terminated Sams Via Electrochemically Triggered Michael Addition: Characterization, Electrochemistry and Complex with Ni(Ii) and Cu(Ii) Cations. *Phys. Chem. Chem. Phys.* **2010**, *12*, 13287−13295.

(27) Zhu, L. J.; Zhu, L. P.; Jiang, J. H.; Yi, Z.; Zhao, Y. F.; Zhu, B. K.; Xu, Y. Y. Hydrophilic and Anti-Fouling Polyethersulfone Ultrafiltration Membranes with Poly(2-Hydroxyethyl Methacrylate) Grafted Silica Nanoparticles as Additive. *J. Membr. Sci.* **2014**, *451*, 157−168.

(28) Eloot, S.; De Vos, J. Y.; De Vos, F.; Hombrouckx, R.; Verdonck, P. Middle Molecule Removal in Low-Flux Polysulfone Dialyzers:

DOI: 10.1021/acsami.5b03951
ACS Appl. Mater. Interfaces 2015, 7, 17748−17755

Impact of Flows and Surface Area on Whole-Body and Dialyzer Clearances. *Hemodial. Int.* **2005**, *9*, 399−408.
(29) Sui, Y.; Wang, Z. N.; Gao, X. L.; Gao, C. J. Antifouling Pvdf Ultrafiltration Membranes Incorporating Pvdf-G-Phema Additive Via Atom Transfer Radical Graft Polymerizations. *J. Membr. Sci.* **2012**, *413*−*414*, 38−47.
(30) Zhao, Y. F.; Zhu, L. P.; Yi, Z.; Zhu, B. K.; Xu, Y. Y. Improving the Hydrophilicity and Fouling-Resistance of Polysulfone Ultrafiltration Membranes Via Surface Zwitterionicalization Mediated by Polysulfone-Based Triblock Copolymer Additive. *J. Membr. Sci.* **2013**, *440*, 40−47.
(31) Zhu, L. P.; Xu, Y. Y.; Dong, H. B.; Yi, Z.; Zhu, B. K. Amphiphilic Ppesk-Graft-P(Pegma) Copolymer for Surface Modification of Ppesk Membranes. *Mater. Chem. Phys.* **2009**, *115*, 223−228.
(32) Yi, Z.; Zhu, L.; Cheng, L.; Zhu, B.; Xu, Y. A Readily Modified Polyethersulfone with Amino-Substituted Groups: Its Amphiphilic Copolymer Synthesis and Membrane Application. *Polymer* **2012**, *53*, 350−358.
(33) Zhao, Y. F.; Zhu, L. P.; Yi, Z.; Zhu, B. K.; Xu, Y. Y. Zwitterionic Hydrogel Thin Films as Antifouling Surface Layers of Polyethersulfone Ultrafiltration Membranes Anchored Via Reactive Copolymer Additive. *J. Membr. Sci.* **2014**, *470*, 148−158.
(34) Song, H.; Ran, F.; Fan, H.; Niu, X.; Kang, L.; Zhao, C. Hemocompatibility and Ultrafiltration Performance of Surface-Functionalized Polyethersulfone Membrane by Blending Comb-Like Amphiphilic Block Copolymer. *J. Membr. Sci.* **2014**, *471*, 319−327.
(35) Qin, H.; Sun, C.; He, C.; Wang, D.; Cheng, C.; Nie, S.; Sun, S.; Zhao, C. High Efficient Protocol for the Modification of Polyethersulfone Membranes with Anticoagulant and Antifouling Properties Via in Situ Cross-Linked Copolymerization. *J. Membr. Sci.* **2014**, *468*, 172−183.

DOI: 10.1021/acsami.5b03951
ACS Appl. Mater. Interfaces 2015, 7, 17748−17755